Supplementary Information

The PPARα - FGF21 hormone axis contributes to metabolic regulation by the hepatic JNK signaling pathway

Santiago Vernia, Julie Cavanagh-Kyros, Luisa Garcia-Haro, Guadalupe Sabio, Tamera Barrett, Dae Young Jung, Jason K. Kim, Jia Xu, Hennady P. Shulha, Manuel Garber, Guangping Gao, and Roger J. Davis

Supplementary Experimental Procedures

Supplementary Figures S1 – S7

Supplementary References

SUPPLEMENTARY EXPERIMENTAL PROCEDURES

Genotyping

PCR assays with genomic DNA and the amplimers 5'-TTACTGACCGTACACCAAATTTGCC TGC-3' and 5'-CCTGGCAGCGATCGCTATTTTCCATGAGTG-3' were used to detect the *Cre*$^{+}$ allele (450 bp). The amplimers 5'CCTCAGGAAGAAAGGGCTTATTTC-3' and 5'-GAACCACTGTTCCAATTTCCATCC-3' detected the *Jnk1*$^{+}$ allele (1,550 bp), the *Jnk1*^{LoxP} allele (1,095 bp), and the *Jnk1*$^{\Delta}$ allele (395 bp). The amplimers 5'- GTTTTGTAAAGGGAGCCGAC -3' and 5'- CCTGACTACTGAGCCTGGTTTCTC -3' were used to detect the *Jnk2*$^{+}$ allele (224 bp) and the *Jnk2*^{LoxP} allele (264 bp). The amplimers 5'- GGAATGTTTGGTCCTTTAG -3', 5'-GCTATTCAGAGTTAAGTG-3', and 5'- TTCATTCTAAGCTCAGACTC -3' were used to detect the *Jnk2*^{LoxP} allele (560 bp) and the *Jnk2*$^{\Delta}$ allele (400 bp).

Immunoblot analysis

Tissue extracts were prepared using Triton lysis buffer (20 mM Tris at pH 7.4, 1% Triton X-100, 10% glycerol, 137 mM NaCl, 2 mM EDTA, 25 mM β-glycerophosphate, 1 mM sodium orthovanadate, 1 mM phenylmethylsulfonyl fluoride, 10 mg/mL of aprotinin and leupeptin). Extracts (20–50 µg of protein) were examined by protein immunoblot analysis by probing with antibodies to NCOR1 and NRIP1 (Abcam), ACC, AKT, phospho-Thr^{308} AKT, and phospho-Ser^{473} AKT (Cell Signaling), FASN and JNK (Pharmigen), pJNK (Cell Signaling), PPARα (Millipore), NCOR2 (Pierce), GAPDH (Santa Cruz) and αTubulin (Sigma). Immune complexes were detected using the Odyssey infrared imaging system (LI-COR Biosciences).

Protein kinase assays

JNK activity was measured using an *in vitro* protein kinase assay with the substrates cJun and [γ-^{32}P]ATP (Whitmarsh and Davis, 2001).

RNA-seq analysis

Hepatic RNA was isolated using the RNeasy kit (Qiagen). RNA quality (RIN > 9) was verified using a Bioanalyzer 2100 System (Agilent Technologies). Total RNA (10µg) pooled from groups of 3 mice were used for the preparation of each RNA-seq library by following the manufacturer's instructions (Illumina). Three independent libraries were examined for each condition. The cDNA libraries were sequenced by Illumina Hi-Seq with a paired-end 40-bp format. Reads from each sample were aligned to the mouse genome (UCSC genome browser mm10 build) using TopHat2 (Kim et al., 2013). The average number of aligned reads per library was > 30,000,000. Hepatic gene expression was quantitated as fragments per kilobase of exon model per million mapped fragments (FPKM) using Cufflinks (Trapnell et al., 2010). Differentially expressed genes were identified using the Cufflinks tools Cuffmerge and Cuffdiff. Gene ontology was examined by Kyoto Encyclopedia of Genes and Genome (KEGG) pathways analysis (Kanehisa et al., 2012) with the Database for Annotation, Visualization and Integrated Discovery (DAVID) (Huang da et al., 2009).

Quantitative RT-PCR analysis of mRNA

The expression of mRNA was examined by quantitative PCR analysis using a Quantstudio PCR machine (Life Technologies). TaqMan® assays were used to quantify *Acadl* (Mm00599660_m1), *Acadm* (Mm00431611_m1), *Acadvl* (Mm00444293_m1), *Acox1* (Mm01246831_m1),

Adiponectin (Mm00456425_m1), *Arg1* (Mm00475988_m1), *Ccl2* (Mm00441242_m1), *Cox7a* (Mm00438296_m1), *Cox8b* (Mm00432648_m1), *Cpt1b* (Mm00487189_g1), *Cyp4a10* (Mm026016990_gH), *Cyp4a14* (Mm00484135_m1), *Cyp4a32* (Mm01730047_g1), *Cyp7b1* (Mm00484157_m1), *Dio1* (Mm00839358_m1), *Dio2* (Mm00515664_m1), *Ehhadh* (Mm00619685_m1), *Emr1* (F4/80) (Mm00802530_m1), *Fgf21* (Mm00840165_m1), *G6pc* (Mm 00839363_m1), *Hadhb* (Mm00695255_g1), *Il1b* (Mm00434228_m1), *Ldhb* (Mm00493146_m1), *Leptin* (Mm00434759_m1), *Lpl* (Mm00434770_m1), *Mgl2* (Mm00460844_m1), *Msr1* (Mm00446214_m1), *Ncor1* (Mm01333102_m1), *Ncor2* (Mm00448796_m1), *Pck1* (Mm01247058_m1), *Pdk4* (Mm01166879_m1), *Pgc1a* (Mm01208835_m1), *Pgc1b* (Mm00504720_m1), *Ppara* (Mm00440939_m1), *Pparg2* (Mm00440940_m1), *Rxra* (Mm01332431_m1), *Tnfa (Mm00443258_m1), Ucp1* (Mm00494069_m1), , The relative mRNA expression was normalized by measurement of the amount of *18S* RNA in each sample using Taqman© assays (catalog number 4308329; Life Technologies).

Quantitative measurement of *Jnk*α/β mRNA was examined by quantitative PCR using the Quantifast probe PCR kit (Qiagen) and the following combination of primers and Taqman probes (Applied Biosystems): *Jnk1*α (Fwd, 5'-GGAGAACGTGGACTTATGGTCTGT-3'; Probe: 5'-6FAM-TGCCACAAAATCCT-MGBNFQ-3'; Rev, 5'-TGATCAATATAGTCCCTTCCTGGAA-3'); *Jnk1*β (Fwd, 5'-GAACGTTGACATTTGGTCAGTTG-3'; Probe, 5'-6FAM-AGAAATGATCAAAGGTGGTGTT-MGBNFQ-3'; Rev, 5'-TCAATATGATCTGTACCTGGGAACA-3'); *Jnk2*α (Fwd, 5'-GGTCAGTGGGTTGCATCATG-3'; Probe, 5'-6FAM-AGCTGGTGAAAGGTT-MGBNFQ-3'; Rev, 5'-TGATCAATATGGTCAGTACCTTGGA-3'); and *Jnk2*β (Fwd, 5'-ATCTGGTCTGTCGGGTGCAT-3'; Probe: 5'-6FAM-AAATGGTCCTCCATAAAG-MGBNFQ-3'; Rev, 5'-GATCAATATAGTCTCTTCCTGGGAACA-3').

Mitochondrial DNA copy number

Genomic DNA was isolated from liver using a DNeasy Blood and Tissue kit (Qiagen). Mitochondrial DNA (mtDNA) copy number was quantified by qPCR from isolated total DNA (Sahin et al., 2011). Briefly, 50 ng of total liver DNA was used in each qPCR reaction and the data obtained were analyzed by the ΔΔCT method. Two different primer pairs were used to quantify and confirm relative mtDNA copy number: *CoxI* and *Cytochrome b* (mitochondrial DNA); and *β-Globin/H-19* (genomic DNA). The amplimers were: COXIF 5'-CTGAGCGGGAATAGTGGGTA-3'; COXIR 5'-TGGGGCTCCGATTATTAGTG-3'; CytBF 5'-ATTCCTTCATGTCGGACGAG-3'; CytBR 5'-ACTGAGAAGCCCCCTCAAAT-3'; H19R 5'-GTCCACGAGACCAATGACTG-3'; H19F 5'-GTACCCACCTGTCGTCC-3'; B1globinF 5'-GCACCTGACTGATGCTGAGAA-3'; B1globinR 5'-TTCATCGGCGTTCACCTTTCC-3'.

Chromatin immunoprecipitation

Frozen livers were pulverized using a CP02 system (Covaris) and then cross-linked in 1.5% formaldehyde in PBS (15 min) at room temperature. The reaction was quenched with 0.125 M glycine. Cross-linked chromatin was prepared using the SimpleChip Plus Enzymatic Chromatin IP kit (Cell Signaling) following the manufacturer's instructions. A portion of the diluted lysates (2%) was reserved as an input control. The remaining lysates were incubated overnight at 4°C with 3 µl of NCoR1 antibody (Abcam), 2.5 µl NRIP1 antibody (Abcam), 2.5 µl H4K16ac histone H4 antibody (Cell Signaling), 2.5 µl of PPARα antibody (Millipore), or 2.5 µl of control IgG per 10^6 cells. The antibodies were captured with protein-G magnetic beads (3h), pelleted, and washed in low salt and high salt buffers provided by the kit. The chromatin was eluted and the crosslinks reversed by heating at 65°C (4h). The chromatin was treated with proteinase K and the purified DNA was used for quantitative PCR analysis. The amplimers FGF21F 5'-AGGGCCCGAATGCTAAGC-3' and FGF21R 5'-AGCCAAGCAGGTGGAAGTCT-3' were used to obtain a 83 bp amplicon encompassing the PPRE of the *Fgf21* gene with SYBR green mix

(Applied Biosystems). Control studies were performed to detect a region of *Gapdh* gene by TaqMan® assay (catalog # 4352339E, Applied Biosystems); no significant enrichment was detected. Quantitative PCR was performed using a Quantstudio 12k flex Real-Time PCR system (Applied Biosystems). Data are presented as fold-change versus 2% input.

Primary hepatocytes

Hepatocytes were isolated from mice using a modified 2-step perfusion method (Seglen, 1976) using Liver Perfusion Media and Liver Digest Buffer (Invitrogen). Cells were seeded on plates (pre-coated (1 h) with collagen I (BD Biosciences)) in DMEM plus 10% FBS, 2mM sodium pyruvate, 1μM dexamethasone, 100 nM insulin plus 2% penicillin/streptomycin. After attachment (2 h), the medium was removed and the hepatocytes were incubated (22 h) in maintenance medium (DMEM (4.5g/L glucose) supplemented with 10% FBS, 0.2% BSA, 2mM sodium pyruvate, 2% Pen/Strep, 0.1 μM dexamethasone, 1nM insulin). When indicated, the hepatocytes were incubated (16 h) with PPARα agonists (50 μM WY14043 (Sigma) or 100 μM Fenofibrate (Sigma)) or antagonists (10 μM GW6471 (Sigma) or 20 μM MK886 (Santa Cruz)) or the JNK inhibitor (E)-3-(4-(dimethylamino)but-2-enamido)-N-(3-methyl-4-((4-(pyridin-3-yl)pyrimidin-2-yl)amino)phenyl)benzamide (JNK-in-8; EMD-Millipore; Zhang et al. (2012)). The drugs were dissolved in DMSO; control studies were performed by addition of vehicle (DMSO) alone.

Glucose production by primary hepatocytes was evaluated incubating $5.5x10^5$ cells in collagen-coated 35 mm wells (6 well plates) with M199 media (Invitrogen) supplemented with 0.5% BSA, 20mM Lactate and 2mM Pyruvate for the indicated times. Glucose production in the medium was assessed using the glucose (HK) assay kit (Sigma) and values were normalized to total hepatocyte protein.

Lactate production was evaluated by incubating $5.5x10^5$ primary hepatocytes in collagen-coated 35 mm wells (6 well plates) with DMEM (4.5 g/L glucose) supplemented with 0.2% BSA, 2% Pen/Strep, 1nM Insulin, and 0.1μM dexamethasone. Lactate production in the medium was assessed using the reconstituted Lactate Reagent (Beckman Coulter) and values were normalized to total hepatocyte protein.

Oxygen consumption

The oxygen consumption rate (OCR) was quantitated using primary hepatocytes with a XF24 Extracellular Flux Analyzer (Seahorse Bioscience) and XF Assay Kits to measure extracellular flux changes of oxygen and protons. Briefly, primary hepatocytes were plated ($4x10^4$ cells/well) in collagen-coated XF24-microplates (Seahorse Bioscience). After attachment (2 h), the hepatocytes were transferred to running medium (sodium bicarbonate-free DMEM (4.5 g/L glucose) supplemented with 0.2% BSA, 2% Pen/Strep, 1nM Insulin and 0.1μM dexamethasone) and incubated at 37°C in a humidified atmosphere without CO_2 supplementation. Baseline measurements were performed prior to addition of substrates (1g/L glucose, 200 μM palmitate-BSA, or 10mM lactate/1mM pyruvate) or inhibitors (1 μM Oligomycin, 0.1 μM FCCP, or 100 nM Rotenone). Mitochondrial oxygen consumption rates were calculated from the difference between the maximal respiratory rate (in the presence of FCCP) and the respiratory rate after addition of rotenone. Data obtained from 10 ~ 11 independent wells were examined for each condition.

Analysis of tissue sections

Histology was performed using tissue fixed in 10% formalin for 24 h, dehydrated, and embedded in paraffin. Sections (7 μm) were cut and stained using hematoxylin and eosin (American Master Tech Scientific). Parafin sections were stained with an antibody to insulin (Dako). The primary antibodies were detected by incubation with anti-guinea pig Ig conjugated

to Alexa Fluor 488 (Invitrogen). DNA was detected by staining with DAPI (Life Technologies). Fluorescence was visualized using a Leica TCS SP2 confocal microscope equipped with a 405-nm diode laser. Islet area was determined by dividing total β cell area (marked by staining with insulin antibodies) by the pancreatic area per section using ImageJ64 software.

Electron microscopy

Transmission electron microscopy was performed using tissue washed with 0.1 M sodium cacodylate buffer (pH 7.2), and fixed with 2.5% gluteraldehyde for 30 min at room temperature and in the same fresh fixative overnight at 4°C. The tissue was then rinsed for 10 min in 0.1 M sodium cacodylate buffer (pH 7.2) three times and then post-fixed (1 h) in 1% (wt/vol) osmium tetroxide in distilled water. The fixed tissue was then rinsed in double distilled water and dehydrated through a graded ethanol series before two changes of ethanol 100%. Samples were then infiltrated first with two changes of 100% propylene oxide and then with a 50%/50% propylene oxide / SPI-Pon 812 resin mixture. The following day three changes of fresh 100% SPI-Pon 812 resin were done before the samples were polymerized at 68°C in flat embedding molds. The epoxy blocks were cut and mounted on blank epoxy stubs with a drop of Super Glue, and ultrathin sections were cut on a Reichart-Jung ultramicrotome using a diamond knife. The sections were collected and mounted on copper support grids, contrasted with lead citrate and uranyl acetate, and examined using a FEI Tecnai 12 BT with 80Kv accelerating voltage, and images were captured using a Gatan TEM CCD camera.

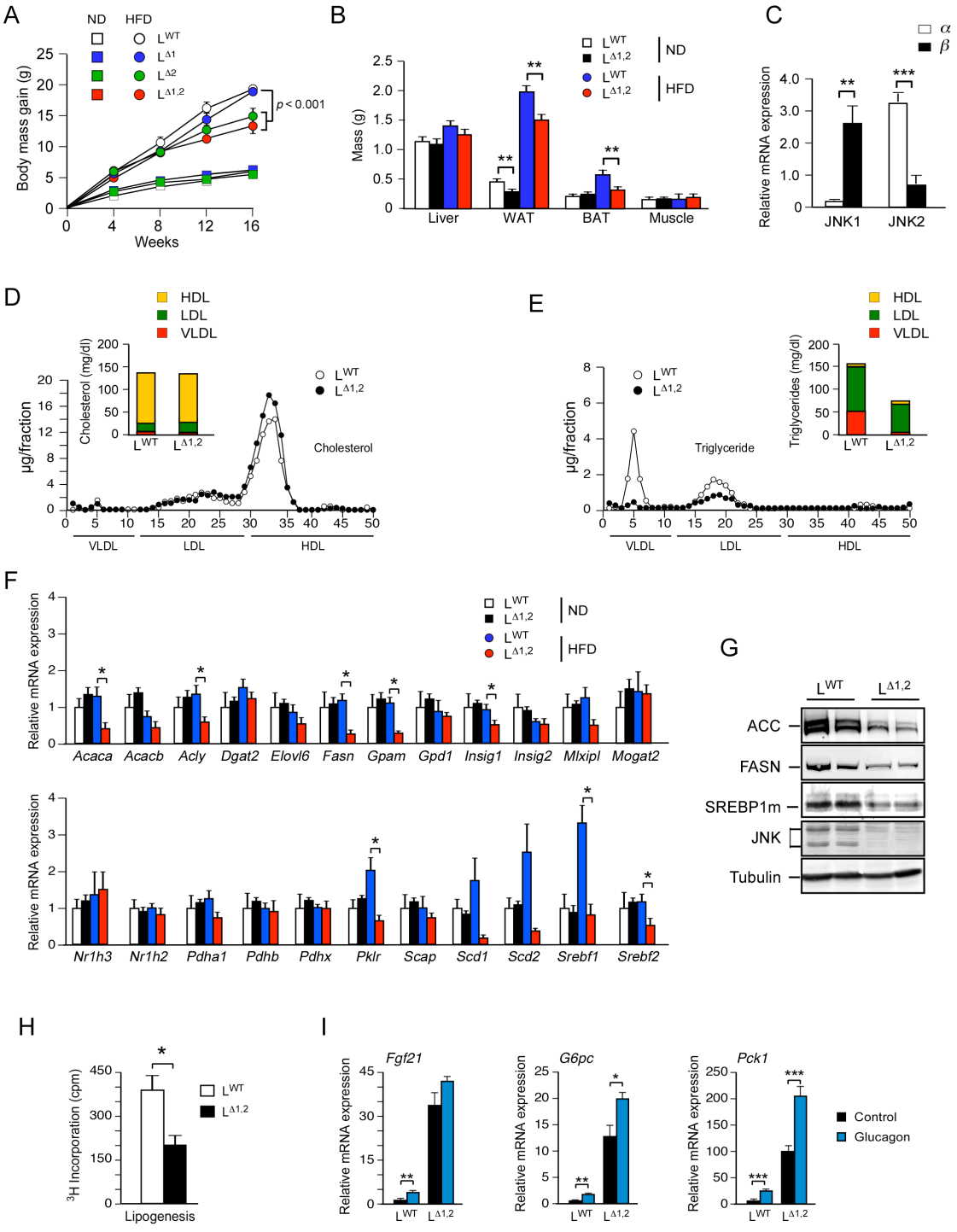

Figure S1. Effect of hepatic JNK-deficiency on body mass and blood lipids, Related to Figure 1.

(**A,B**) Mice were fed a chow diet (ND) or a HFD. The time course of body mass gain (A) and organ mass at necropsy at 16 wk (B) is presented (mean ± SEM; n = 25 ~ 30; **, $p < 0.01$).

Key: White adipose tissue (WAT); brown adipose tissue (BAT), gastrocnemius muscle (Muscle).

(**C**) The expression of the α and β isoforms of *Jnk1* and *Jnk2* mRNA were measured by quantitative RT-PCR analysis of hepatic RNA (mean ± SEM; n = 8; **, $p < 0.01$; ***, $p < 0.001$).

(**D,E**) Blood lipoproteins were examined by FPLC analysis of cholesterol (E) and triglyceride (F) of serum obtained from 5 mice.

(**F**) The hepatic expression of genes related to lipogenesis was measured by RNA-seq analysis and is presented as the mean ± SEM (n = 3) of data obtained from L^{WT} and $L^{\Delta 1,2}$ mice fed (16 wk) a chow diet or a HFD. Statistically significant differences between L^{WT} and $L^{\Delta 1,2}$ mice are indicated (*, $p < 0.05$).

(**G**) Hepatic expression of ACC, FASN, SREBP1m, JNK, and α-Tubulin was examined by immunoblot analysis of HFD-fed (16 wks) L^{WT} and $L^{\Delta 1,2}$ mice.

(**H**) Hepatic lipogenesis by L^{WT} and $L^{\Delta 1,2}$ mice was measured by examining the incorporation of $^3H_20$ into lipids (mean ± SEM; n = 3; *, $p < 0.05$).

(**I**) Primary cultures of L^{WT} and $L^{\Delta 1,2}$ hepatocytes were incubated (8 h) without or with 50 nM glucagon. The expression of *Fgf21*, *G6pc*, and *Pck1* mRNA was examined by quantitative RT-PCR assays (mean ± SEM; n = 6; *, $p < 0.05$; **, $p < 0.01$; ***, $p < 0.001$).

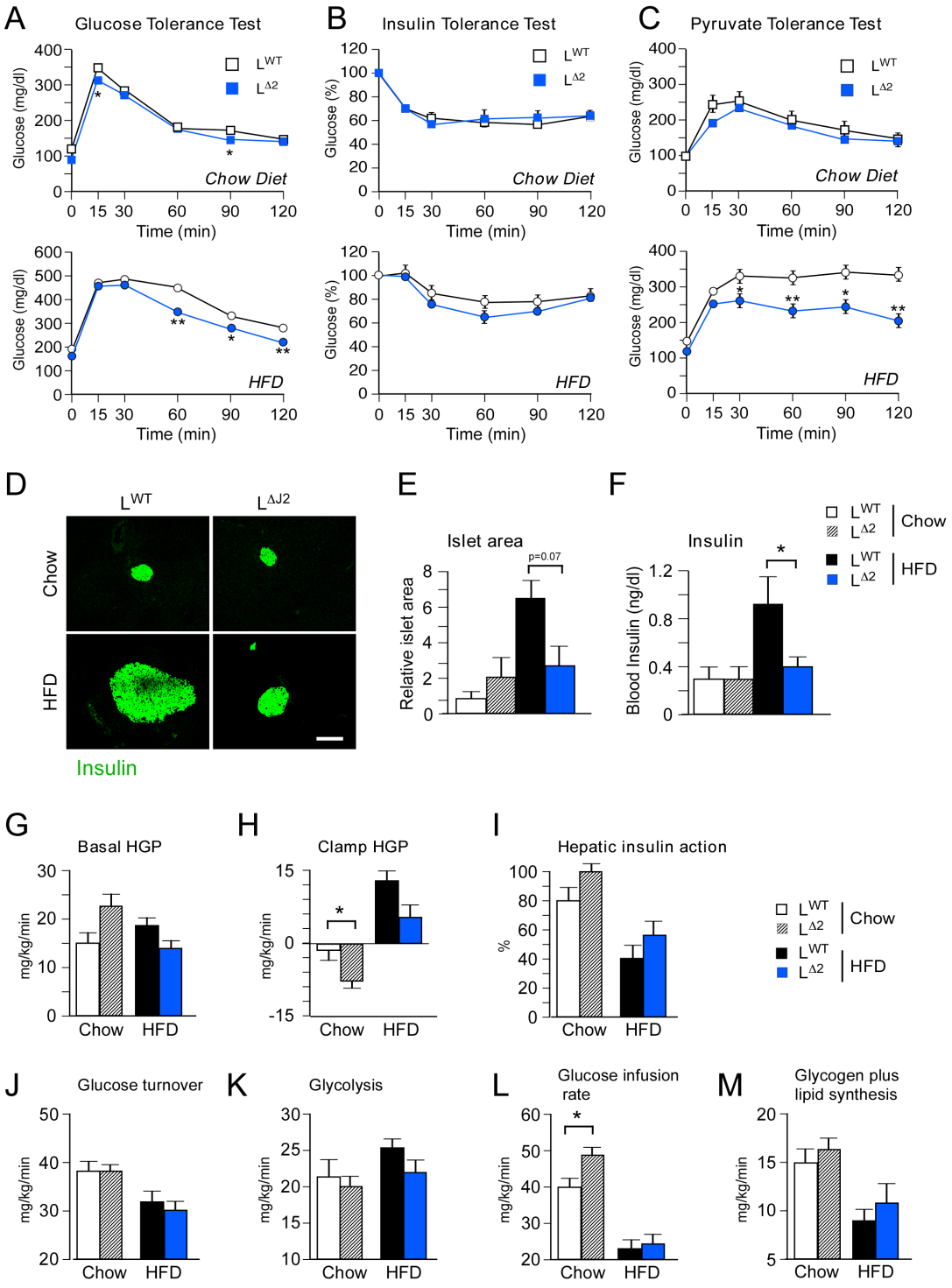

Figure S2. Effect of hepatic JNK2-deficiency on glycemia, Related to Figure 1.

(**A-C**) Glucose (A), insulin (B), and pyruvate (C) tolerance tests were performed on mice fed (16 wk) a chow diet or a HFD (mean ± SEM; n = 20 ~ 50; *, $p < 0.05$; **, $p < 0.01$).

(**D**) Mice were fed a chow diet or a HFD (16 wk). Sections of the pancreas were stained with an antibody to insulin. Bar, 100 μm.

(**E**) Relative islet size was measured using Image J64 software (mean ± SEM; n = 30).

(**F**) The mice were fasted overnight and the blood concentration of insulin was measured (mean ± SEM; n = 16; *, $p < 0.05$).

(**G-M**) Insulin sensitivity was measured using hyperinsulinemic-euglycemic clamps in conscious L^{WT} and $L^{\Delta 2}$ mice fed (4 wk) a chow diet or a HFD. (**G**) Basal hepatic glucose production (HGP). (**H**) HGP during the clamp. (**I**) Hepatic insulin action, expressed as insulin-mediated percent suppression of basal HGP. (**J**) Whole body glucose turnover. (**K**) Whole body glycolysis. (**L**) Glucose infusion rate. (**M**) Glycogen plus lipid synthesis. The data presented are the mean ± SEM for 6 experiments; * $p < 0.05$).

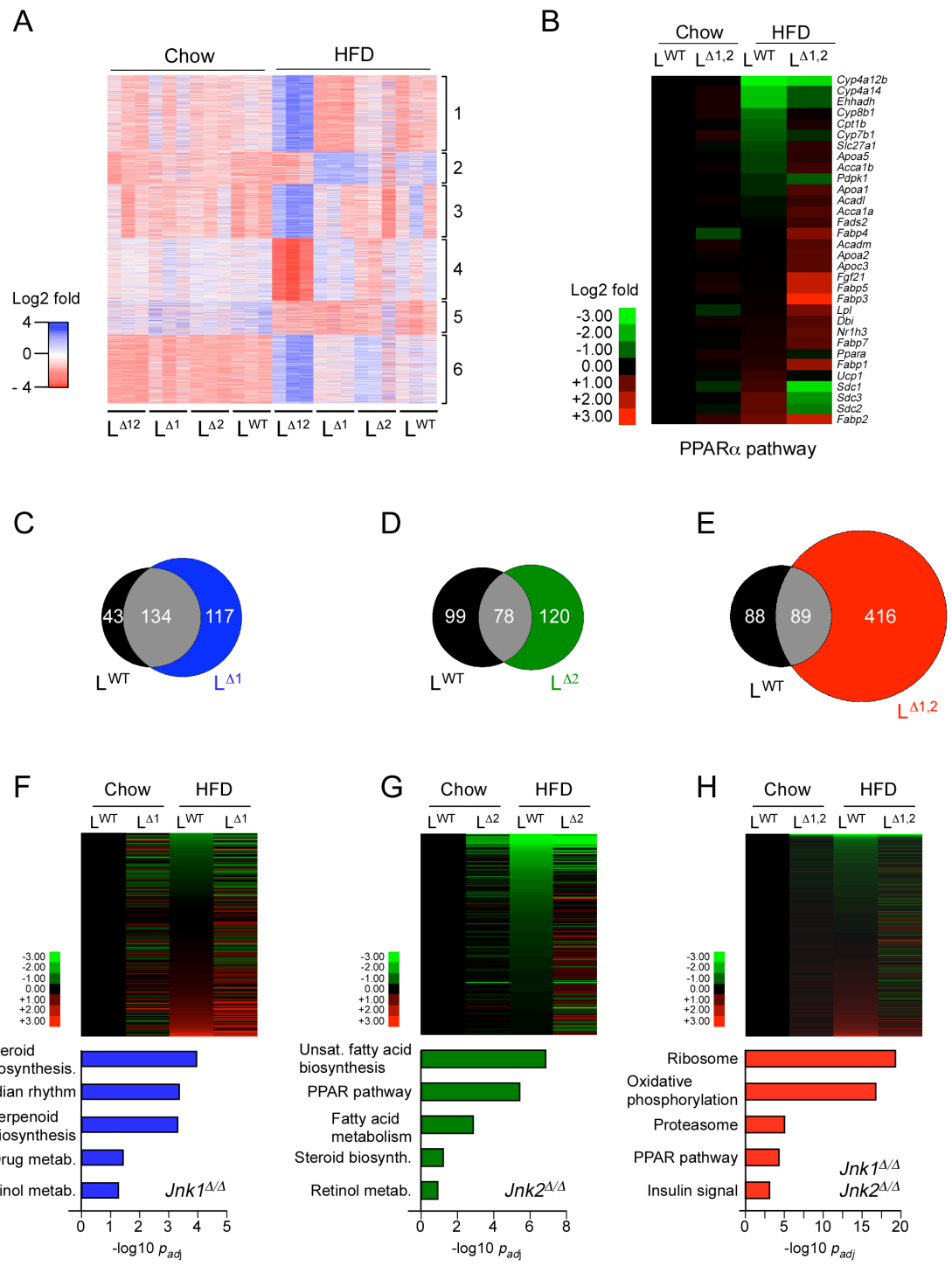

Figure S3. Analysis of hepatic genes differentially regulated by high fat diet in control and liver-specific JNK-deficient mice, Related to Figure 3.

(**A**) RNA-seq analysis was performed on three independent libraries prepared from control and liver-specific JNK-deficient mice fed a chow diet or a HFD (16 wks) and starved overnight.

Differentially expressed genes (log2 fold ratio ≥ 0.75; FKPM > 10) were examined by k-means (k = 6) clustering and displayed as a heatmap. KEGG pathway enrichment identified by gene ontology analysis was identified for each gene cluster: 1) oxidative phosphorylation and ribosomes; 2) drug metabolism; 3) oxidative phosphorylation and ribosomes; 4) no significant KEGG pathway enrichment ($p > 0.01$); 5) retinol metabolism and steroid hormone biosynthesis; and 6) PPAR signaling pathway.

(**B**) Hepatic gene expression related to the PPARα pathway is presented as a heatmap of RNA-seq data (mean, n = 3) obtained from L^{WT} and $L^{\Delta 1,2}$ mice fed a chow diet or a HFD (16 wk). The genes are displayed with lowest expression (*top*) to highest expression (*bottom*) in HFD-fed L^{WT} liver. The scale represents log2 fold change compared with chow-fed L^{WT} mice.

(**C-E**) Genes that were differentially expressed between mice fed a chow diet were defined as those genes that have a log2 fold ratio of 1.5 and a Benjamin-Hochberg FDR corrected *p* (p_{adj}) value < 0.01 when compared to hepatic gene expression in control mice (FPKM ≥ 10 and length ≥ 200 bp). These differentially expressed genes in mice with hepatic JNK-deficiency ($L^{\Delta 1}$, $L^{\Delta 2}$, or $L^{\Delta 1,2}$) were compared with control L^{WT} mice and presented as Venn diagrams.

(**F-H**) Genes that are differentially expressed ($p_{adj} < 0.01$) between HFD-fed control mice (L^{WT}) and HFD-fed liver-specific JNK-deficient mice ($L^{\Delta 1}$, $L^{\Delta 2}$, or $L^{\Delta 1,2}$) are presented as a heatmap (*upper panel*). The genes are displayed with lowest expression (*top*) to highest expression (*bottom*) in HFD-fed L^{WT} liver. The scale represents log2 fold change compared with chow-fed L^{WT} mice. Gene ontology analysis to identify KEGG pathway enrichment is presented (*lower panel*).

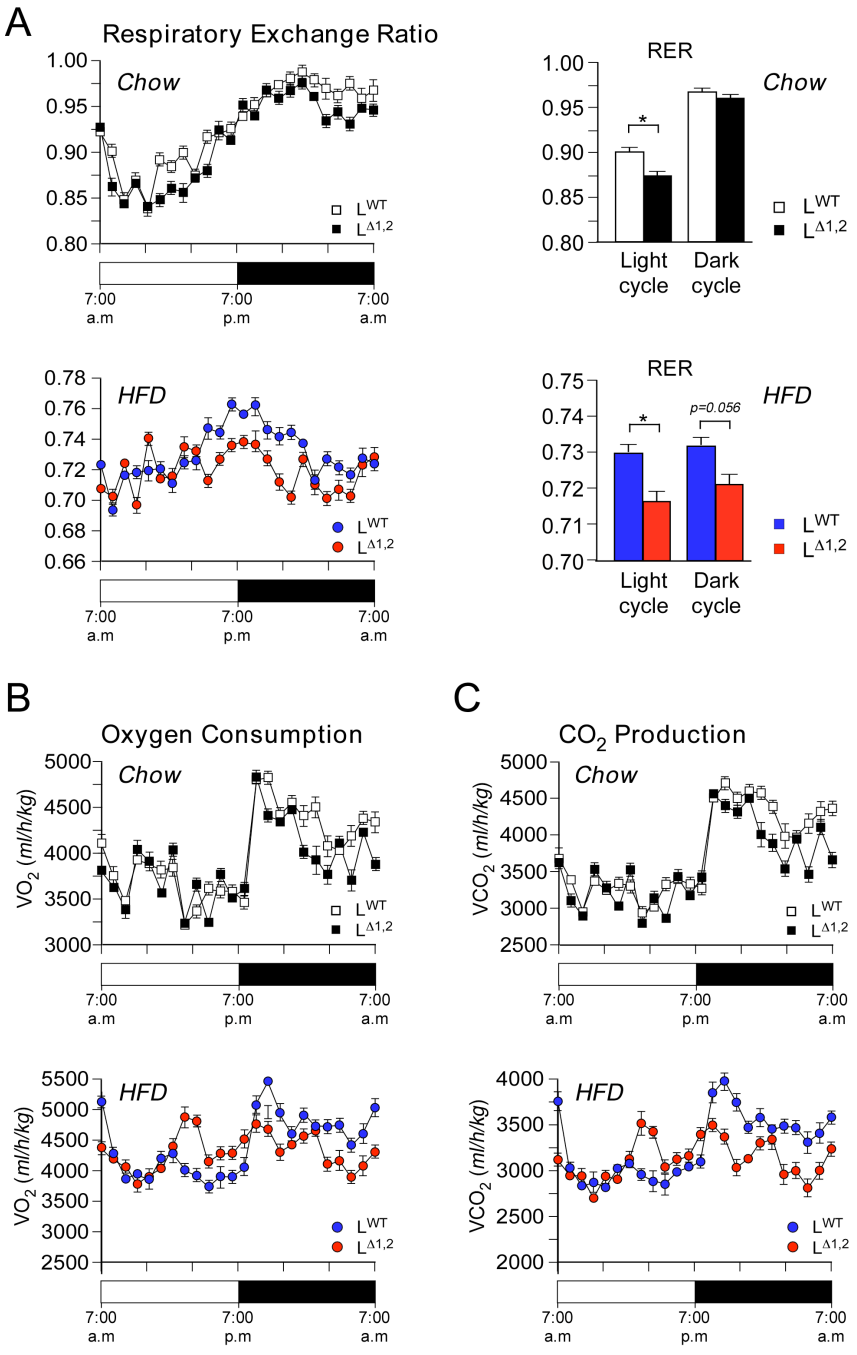

Figure S4. Effect of hepatic JNK-deficiency on oxygen consumption and carbon dioxide production, Related to Figure 3.

(**A**) Metabolic cage analysis of chow-fed and HFD-fed (4 wks) mice was performed. The respiratory exchange ratios of L^{WT} and $L^{\Delta 1,2}$ mice are presented as the mean ± SEM (n = 6; *, $p < 0.05$).

(**B,C**) Oxygen consumption (V_{O2}) and carbon dioxide production (V_{CO2}) by L^{WT} and $L^{\Delta 1,2}$ mice are presented as the mean ± SEM (n = 6).

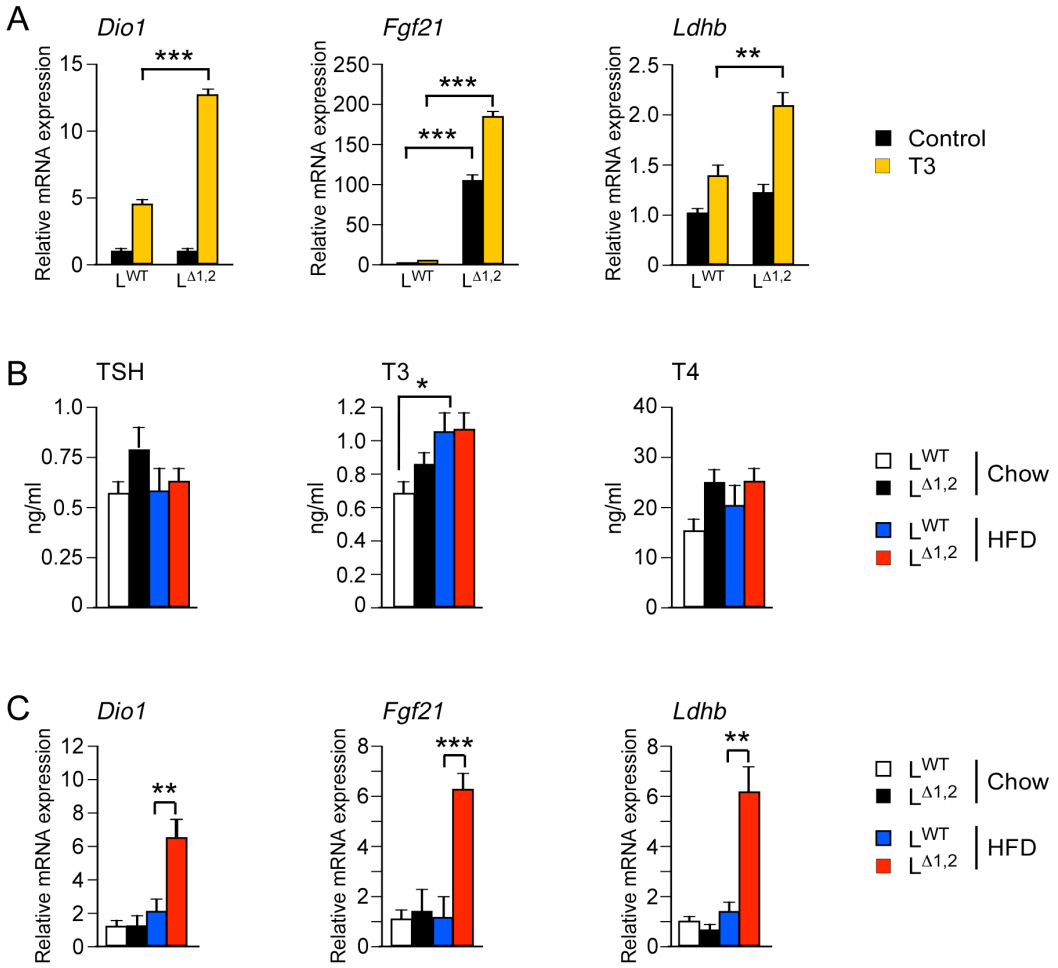

Figure S5. Hepatic JNK-deficiency causes increased thyroid hormone-stimulated gene expression, Related to Figure 5.

(**A**) Primary cultures of L^{WT} and $L^{\Delta 1,2}$ hepatocytes were incubated (16 h) without or with 100 nM triiodothyronine (T3). The expression of *Dio1*, *Fgf21*, and *Ldhb* mRNA was examined by quantitative RT-PCR assays (mean ± SEM; n = 6; **, $p < 0.01$; ***, $p < 0.001$).

(**B**) L^{WT} and $L^{\Delta 1,2}$ mice were fed a chow diet or a HFD (16 wks). The serum concentration of TSH, T3, and T4 was measured (mean ± SEM; n = 8; * $p < 0.05$). No statistically significant differences between L^{WT} and $L^{\Delta 1,2}$ mice were detected ($p > 0.05$).

(**C**) Hepatic JNK-deficiency causes increased expression of thyroid hormone target genes *in vivo*. L^{WT} and $L^{\Delta 1,2}$ mice were fed a chow diet or a HFD (16 wks). The expression of *Dio1*, *Fgf21*, and *Ldhb* mRNA was examined by quantitative RT-PCR assays (mean ± SEM; n = 8; **, $p < 0.01$; ***, $p < 0.001$).

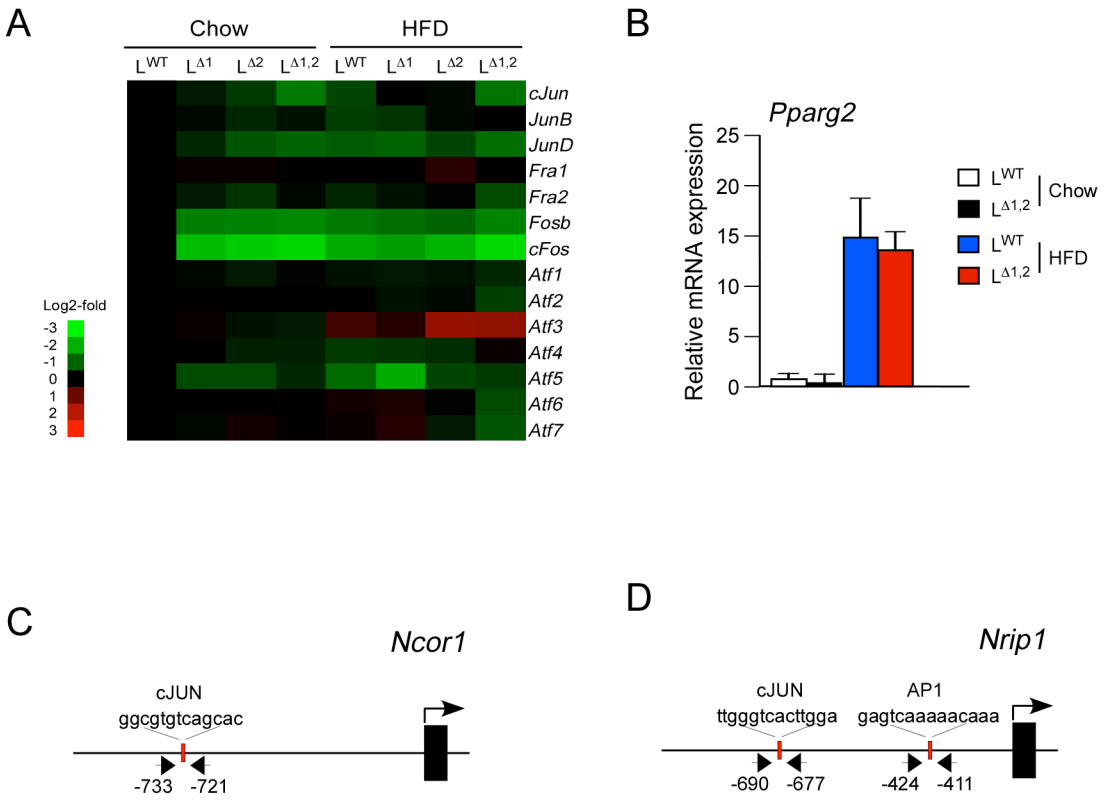

Figure S6. Effect of hepatic JNK-deficiency on the hepatic expression of AP1-related transcription factors and PPARγ2, Related to Figure 5.

(**A**) Control (L^{WT}) mice and hepatic JNK-deficient ($L^{\Delta 1}$, $L^{\Delta 2}$, and $L^{\Delta 1,2}$) mice were fed a chow diet or a HFD (16 wks) and then starved overnight. The expression of AP1-related transcription factor mRNA in the liver was examined by RNA-seq (Fig. S2) and displayed as a heatmap.

(**B**) The expression of *Pparg2* mRNA in the liver of L^{WT} and $L^{\Delta 1,2}$ mice was examined by quantitative RT-PCR analysis of mRNA (mean ± SEM; n = 8). No statistically significant differences between L^{WT} and $L^{\Delta 1,2}$ mice were detected.

(**C**,**D**) Schematic illustration of the proximal 1 kb promoter region of the *Ncor1* (C) and *Nrip1* (D) genes. AP1-related transcription factor binding sites identified using TRANSFAC (http://www.biobase.de) are indicated.

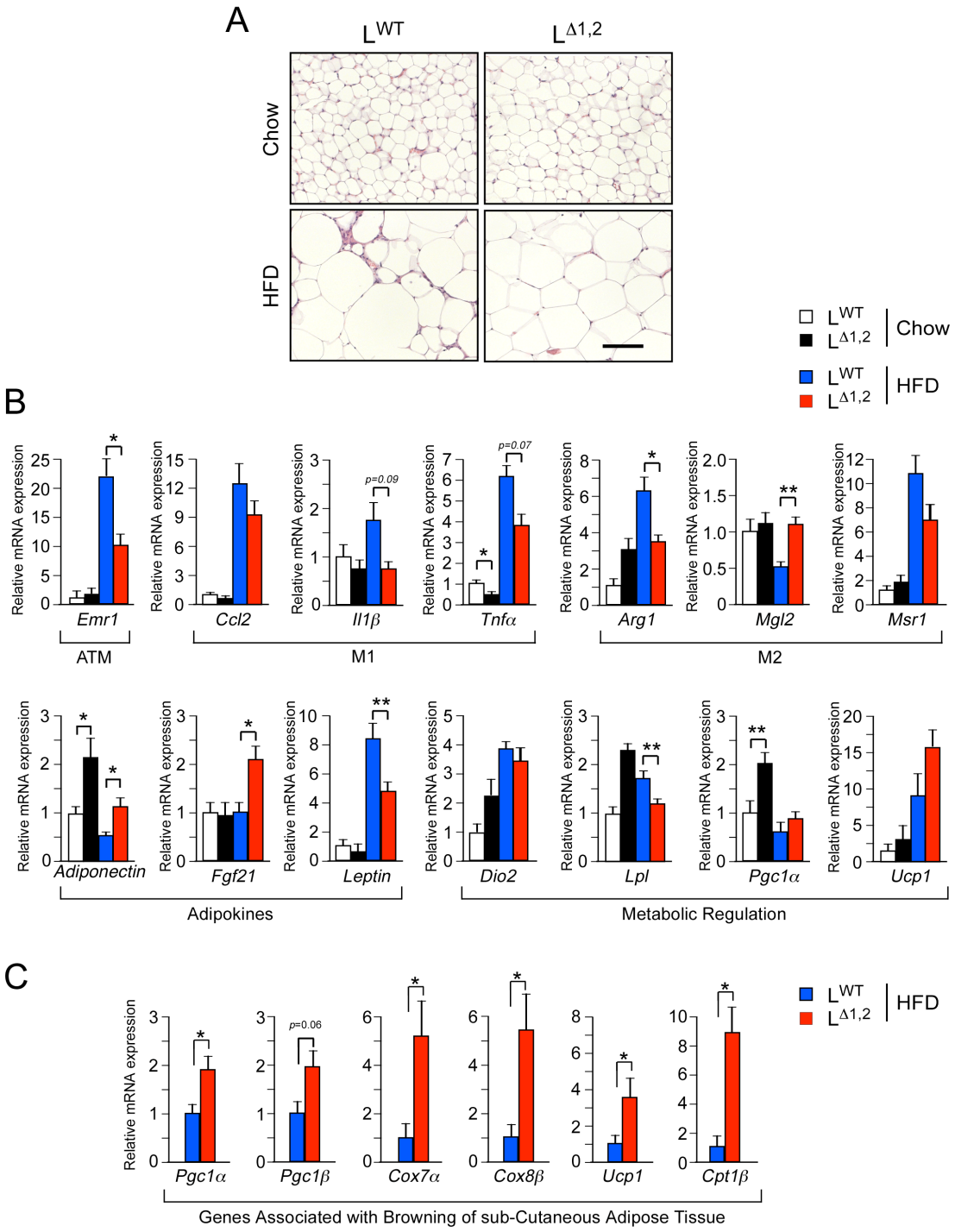

Figure S7. Effect of hepatic JNK-deficiency on adipose tissue, Related to Figure 6.

(**A**) L^{WT} and $L^{\Delta 1,2}$ mice were fed a chow diet or a HFD (16 wks) and then starved overnight. Sections of epididymal adipose tissue were prepared and stained with H & E. Scale bar, 100μm.

(**B**) Epididymal adipose tissue gene expression was measured by quantitative RT-PCR analysis of mRNA (mean ± SEM; n = 8; *, $p < 0.05$; **, $p < 0.01$).

(**C**) L^{WT} and $L^{\Delta 1,2}$ mice were fed a chow diet or a HFD (16 wks) and then starved overnight. Inguinal adipose tissue gene expression was measured by quantitative RT-PCR analysis of mRNA (mean ± SEM; n = 8; *, $p < 0.05$).

SUPPLEMENTARY REFERENCES

Huang da, W., Sherman, B.T., and Lempicki, R.A. (2009). Systematic and integrative analysis of large gene lists using DAVID bioinformatics resources. Nature Protocols *4*, 44-57.

Kanehisa, M., Goto, S., Sato, Y., Furumichi, M., and Tanabe, M. (2012). KEGG for integration and interpretation of large-scale molecular data sets. Nucleic Acids Research *40*, D109-114.

Kim, D., Pertea, G., Trapnell, C., Pimentel, H., Kelley, R., and Salzberg, S.L. (2013). TopHat2: accurate alignment of transcriptomes in the presence of insertions, deletions and gene fusions. Genome Biology *14*, R36.

Sahin, E., Colla, S., Liesa, M., Moslehi, J., Muller, F.L., Guo, M., Cooper, M., Kotton, D., Fabian, A.J., Walkey, C*., et al.* (2011). Telomere dysfunction induces metabolic and mitochondrial compromise. Nature *470*, 359-365.

Seglen, P.O. (1976). Preparation of isolated rat liver cells. Methods in Cell Biology *13*, 29-83.

Trapnell, C., Williams, B.A., Pertea, G., Mortazavi, A., Kwan, G., van Baren, M.J., Salzberg, S.L., Wold, B.J., and Pachter, L. (2010). Transcript assembly and quantification by RNA-Seq reveals unannotated transcripts and isoform switching during cell differentiation. Nature Biotechnology *28*, 511-515.

Whitmarsh, A.J., and Davis, R.J. (2001). Analyzing JNK and p38 mitogen-activated protein kinase activity. Methods Enzymol *332*, 319-336.

Zhang, T., Inesta-Vaquera, F., Niepel, M., Zhang, J., Ficarro, S.B., Machleidt, T., Xie, T., Marto, J.A., Kim, N., Sim, T*., et al.* (2012). Discovery of potent and selective covalent inhibitors of JNK. Chemistry & Biology *19*, 140-154.